Research Square

Preprints are preliminary reports that have not undergone peer review.
They should not be considered conclusive, used to inform clinical practice,
or referenced by the media as validated information.

# An Integrated IoT-Based Predictive Maintenance Framework for Industrial Electrical Assets: A Hybrid Deep Learning Approach

**Hüseyin Yanık**

huseyinyanik@mersin.edu.tr

Mersin Üniversitesi

**Erkan Ödemiş**

Cukurova University

**Yetkin Tongar Serimer**

MIOTE Inc.

**Huzeyfe Doğrukan**

Enerjisa Energy Inc.

**Article**

**Keywords:** Predictive Maintenance, Industrial IoT, Machine Learning, Harmonic Analysis, Motor Current Signature Analysis, Energy Efficiency

**Posted Date:** July 6th, 2026

**DOI:** https://doi.org/10.21203/rs.3.rs-10117105/v1

**License:** This work is licensed under a Creative Commons Attribution 4.0 International License.
Read Full License

**Additional Declarations:** No competing interests reported.

# An Integrated IoT-Based Predictive Maintenance Framework for Industrial Electrical Assets: A Hybrid Deep Learning Approach

**Authors:**

Hüseyin YANIK[1], Erkan ÖDEMİŞ[2], Yetkin Tongar SERİMER[3], Huzeyfe DOĞRUKAN[4]

**Affiliations:**

[1] Department of Information Systems and Technologies, Mersin University, Mersin, Turkey

[2] Department of Biomedical Engineering, Çukurova University, Adana, Turkey

[3] MIOTE Inc., Mersin Technoscope, Mersin, Turkey

[4] ENERJİSA Energy Inc., Ankara, Turkey

HY: orcid.org/0000-0002-4386-5536

EÖ: orcid.org/0000-0003-0212-4288

**Corresponding Author:**

Hüseyin YANIK, Ph.D.

Mersin University Department of Information Systems and Technologies

33343, Mersin, Turkey

**Tel**: +90 553 165 37 44

**E-mail:** huseyinyanik@mersin.edu.tr

**Keywords**: Predictive Maintenance, Industrial IoT, Machine Learning, Harmonic Analysis, Motor Current Signature Analysis, Energy Efficiency

# An Integrated IoT-Based Predictive Maintenance Framework for Industrial Electrical Assets: A Hybrid Deep Learning Approach

**Abstract:** The reliable operation of industrial electrical assets, such as induction motors and distribution transformers, is critical for maintaining production continuity and energy efficiency. Despite advancements in Predictive Maintenance (PdM), existing approaches often rely on isolated sensing modalities and fragmented decision-making processes. This paper presents an integrated IoT-based PdM assistant that leverages high-resolution electrical and harmonic multivariate signatures to detect both electrical and electromechanical incipient faults. The proposed system features an analyzer-grade IoT sensing platform capable of 8 kHz sampling, ensuring IEC 61000-4-30 Class S measurement accuracy. A multilayer feature engineering framework expands 67 primary electrical measurements into a 328-dimensional derived feature space. Furthermore, a hybrid time-series anomaly detection pipeline that combines Prophet for baseline trend modeling with LSTM networks for residual sequence analysis is introduced. Experimental validation conducted over four months on critical cooling-group motors at an industrial facility demonstrates the system's efficacy. Results indicate that the AI-driven module significantly outperforms traditional rule-based alarms in early fault detection. Notably, spectral analysis revealed a correlation between elevated trends in the 5th and 11th harmonics and mechanical bearing degradation, while phase imbalance analysis identified loose connections. The system also quantified energy inefficiencies, estimating annual losses equivalent to 27-28 tons of CO2 emissions, due to high harmonic distortion. The proposed framework offers a comprehensive, explainable, and scalable solution for industrial PdM, bridging the gap between electrical signature analysis and actionable maintenance strategies.

**Keywords:** Predictive Maintenance, Industrial IoT, Machine Learning, Harmonic Analysis, Motor Current Signature Analysis, Energy Efficiency.

## Statements and Declarations

**Competing Interests and Funding:** This study is supported by Türkiye Bilimsel ve Teknolojik Araştırma Kurumu (TÜBİTAK) with a grant number of 7240082.

# 1. Introduction

Induction motors (IMs) and distribution transformers constitute the electromechanical backbone of industrial production lines owing to their robustness, energy efficiency, and comparatively low maintenance requirements [1], [2]. Despite their maturity, unplanned outages originating from incipient electrical or electromechanical faults still inflict substantial direct (spare parts, labor) and indirect (lost throughput, quality deviations, energy overconsumption) costs on manufacturing and utility operators [3]. An electrical fault is characterized by current and voltage levels exceeding the normal operating parameters during power transmission [4], [5]. Such faults can arise from a wide range of causes, including equipment malfunctions, adverse environmental conditions, or human error [6], [7]. Electrical faults can result in substantial economic losses and pose critical safety risks [8]. Typical degradation and fault modes in IMs and related electrical assets include: stator winding insulation breakdown or inter-turn short circuits; rotor faults (cracked or broken bars, dynamic or static eccentricity); bearing wear and lubrication failures; air-gap irregularities; supply and grid-induced disturbances (voltage imbalance, sags/swells, harmonic distortion); and thermal overstress leading to accelerated insulation aging [9], [10], [11], [12]. Therefore, a wide range of methods have been employed in the literature to detect faults in IMs [3].

Conventional condition monitoring and fault detection approaches in industrial systems rely on a range of sensing and diagnostic techniques designed to capture different aspects of equipment degradation and operational anomalies [13]. Among the most widely adopted methods are vibration and acoustic emission analyses, which are commonly used to detect mechanical looseness, bearing defects, and other structural abnormalities in rotating machinery [14]. Thermal monitoring techniques, including infrared imaging and temperature profiling, are also frequently employed to identify localized overheating and load asymmetry that may indicate incipient faults or inefficient operating conditions [15]. In the electrical domain, Motor Current Signature Analysis (MCSA) has been extensively applied to detect rotor bar defects, rotor eccentricity, and certain bearing-related spectral sidebands by analyzing characteristic frequency components in stator current signals [16]. Additionally, insulation-related degradation mechanisms are often assessed through partial discharge measurements and insulation integrity tests, which provide critical insights into stator health and long-term reliability [17].

While effective, several of these methods entail additional sensor installation, mounting constraints, periodic manual acquisition, or limited scalability across geographically distributed assets [9]. Conversely, electrical signatures (currents, voltages, power factors, harmonic spectra) can often be captured non-intrusively from existing panels or compact add-on analyzers, enabling continuous high-granularity coverage with lower marginal cost [18].

Alternatively, Predictive Maintenance (PdM) is an effective strategy for preventing faults [19]. Especially, Industry 4.0 advances have accelerated the convergence of Internet of Things (IoT) telemetry, scalable cloud/edge data infrastructures, and Artificial Intelligence (AI) to transition from reactive or preventive to PdM paradigms [20], [21]. In this approach, machine condition is continuously monitored in real time using sensors and data processing units to enable early fault detection and enhance the operational reliability and efficiency of IMs [22]. Time-stamped multivariate data streams, which are frequently utilized in PdM approaches, provide specialized architectural frameworks that (i) ensure reliable, low-latency acquisition, (ii) normalize and align heterogeneous sampling cadences, (iii) detect anomalies early, and (iv) translate prognostic outputs

into actionable maintenance scheduling [23]. Deep learning sequence models (e.g., LSTM networks) effectively learn temporal dependencies in complex electrical loads [24]. In contrast, decompositional time-series techniques (e.g., Prophet) offer interpretability by isolating trend and seasonal components, facilitating stakeholder trust and root-cause reasoning [25]. Integrating these complementary model families can elevate both predictive accuracy and operational explainability, which is essential in high-risk industrial contexts.

Despite the substantial body of research on predictive maintenance (PdM), several important gaps remain in the existing literature. First, many studies tend to address fault detection, anomaly identification, or maintenance forecasting as isolated tasks [15]. However, only a limited number of works attempt to integrate early anomaly detection, maintenance action recommendation, and energy performance optimization within a single operational framework, resulting in fragmented decision-making processes [26], [27]. Second, the majority of current approaches rely heavily on vibration and thermal monitoring techniques, while high-resolution electrical and harmonic multivariate signatures remain comparatively underutilized as primary sensing modalities [28]. This limitation is particularly notable given their potential to simultaneously capture both mechanical and electrical incipient faults in scalable PdM applications.

Another notable gap concerns the integration of decision-support layers. Existing research rarely addresses the joint optimization of fault severity scoring, residual risk horizon estimation, and the attribution of energy or power quality losses within a unified prioritization framework [29], [30]. Furthermore, hybrid time-series modeling strategies remain relatively underexplored. In particular, the combined use of interpretable decompositional models, such as Prophet, together with deep recurrent or attention-based architectures for residual anomaly segmentation is still an emerging direction. Finally, standards-aligned and region-specific PdM implementations are sparsely documented in the literature [31]. Comprehensive solutions that are explicitly designed to comply with both international standards (e.g., IEC 61000 series) and national distribution or analyzer specifications, while simultaneously generating AI-driven maintenance advisories, remain limited to a small number of reported studies [32], [33].

Addressing the aforementioned gaps, this paper presents an integrated IoT-based PdM assistant for industrial electrical assets (e.g., motors, pumps, and distribution transformers). The main contributions of this study can be summarized as:

- An analyzer-grade IoT sensing platform for high-resolution electrical monitoring, capable of 8 kHz sampling and target Class S measurement accuracy for voltage, current, power, and harmonic metrics, enabling early detection of subtle electrical and electromechanical anomalies.
- A multilayer electrical feature engineering framework that expands a core set of approximately 67 primary electrical measurements into a 328-dimensional derived feature space capturing harmonic behavior, phase imbalance, efficiency indicators, and temporal dynamics, thereby enhancing diagnostic separability for complex fault patterns.
- A hybrid time-series anomaly detection and forecasting pipeline that combines interpretable decompositional forecasting (Prophet) for baseline trend and seasonality modeling with LSTM-based residual sequence analysis to quantify anomaly intensity and detect subtle operational deviations.

- An explainable maintenance decision layer that translates anomaly indicators (e.g., normalized residuals, drift gradients, and multivariate density deviations) into prioritized maintenance actions (Immediate, Planned, or Monitor), while simultaneously linking detected anomalies to power quality degradation and energy efficiency losses such as power factor deviation, reactive power imbalance, and harmonic escalation.

The remainder of the paper is structured as follows: Section 2 details the system architecture (hardware design, communication stack, data model). Section 3 explains the hybrid anomaly detection and forecasting methodology. Section 4 presents the experimental setup, datasets, evaluation metrics, and results from an industrial deployment. Section 5 discusses findings, limitations, and comparison with conventional approaches. Section 6 concludes and outlines future research directions.

# 2. Methodology

## 2.1. System Architecture Overview

As illustrated in Figure 1, an end-to-end architecture has been developed that monitors the pre-failure behavior of industrial electrical equipment using electrical signatures and converts this data into predictive maintenance. The architecture consists of: (a) embedded hardware with standardized measurement accuracy and high harmonic resolution, (b) MQTT-based telemetry that is resilient to industrial conditions and has low latency, (c) a scalable server and database layer suitable for time series data, and (d) a hybrid anomaly–predictive pipeline. The design principles are determined by data quality and continuity requirements that enable continuous monitoring and early anomaly visibility in the field, targeting IEC 61000-4-30 Class S accuracy.

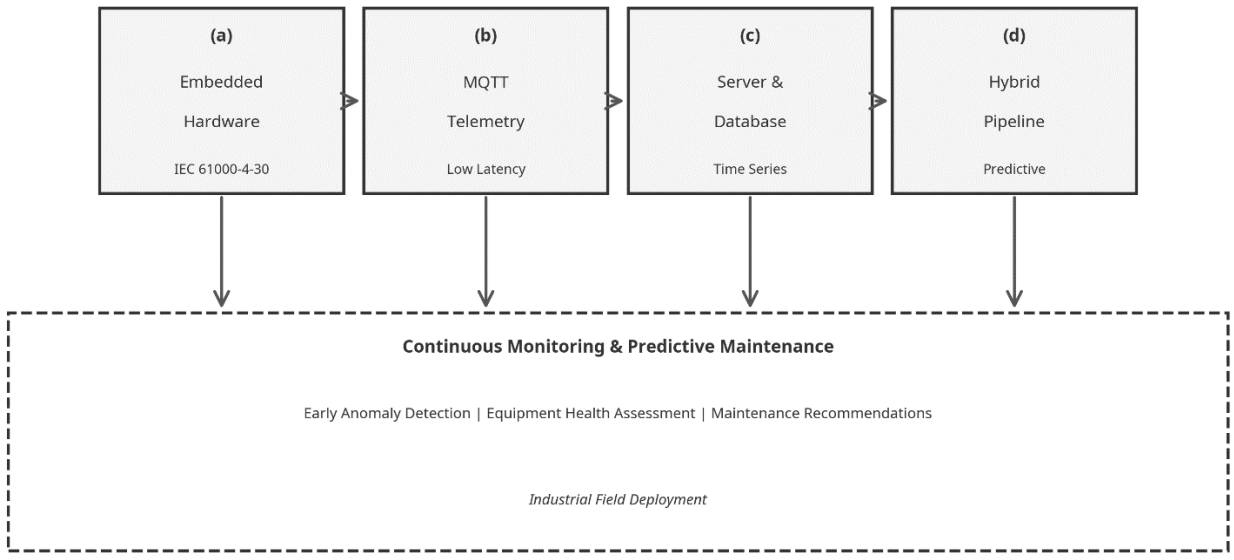



**Fig. 1:** Architecture of the developed system showing the integrated measurement module, communication module, microcontroller, and MQTT-based telemetry stack.

## 2.2. Hardware Design and Subsystems

The hardware design of the measurement probe, depicted in Figure 2, is based on the ADE9000 integrated circuit, which provides power quality and energy parameters in a single package. The line voltage is scaled to approximately 333 mV RMS via a voltage divider to match the integrated input range; a current transformer with a 5 A secondary is used for current measurement, selected to match the industrial load capacity. The secondary signal is converted to the millivolt range at a ratio of 1000:1 using ZMCT103C, and the voltage induced across 66 $\Omega$ is brought to approximately 330 mV, then sampled by the ADE9000. Filtering and noise-suppression steps were applied in the analog conditioning chain to limit aliasing, and configuration and high-reliability data reading were provided via SPI on the digital interface.

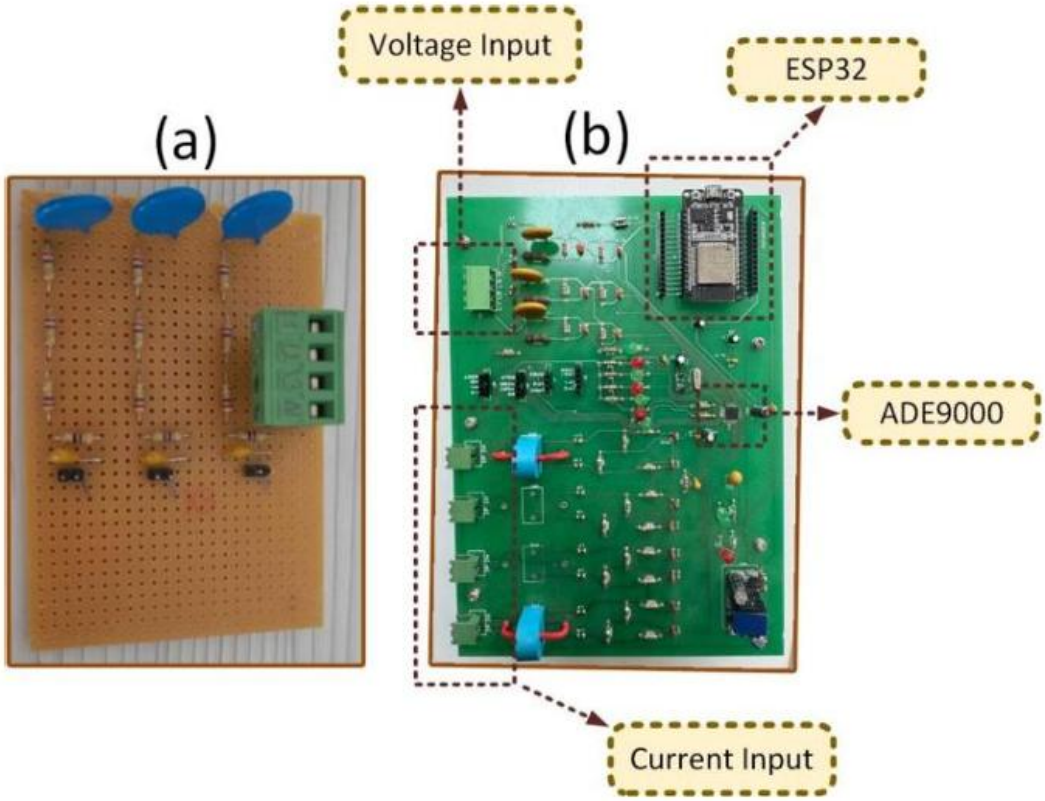



**Fig. 2:** (a) Voltage divider circuit and (b) Sample electronic card design with ADE9000, ESP32, and signal conditioning components.

The ESP32 microcontroller serves as the core processing unit at the edge, managing the MQTT-based telemetry and buffering logic as shown in Figure 3. The ESP32 was specifically selected for its dual-core Tensilica Xtensa LX6 microprocessor, which enables concurrent execution of data-acquisition and network-communication tasks. Operating at 240 MHz, it provides sufficient computational power to perform initial signal validation, basic filtering, and data packetization before transmission. Furthermore, its integrated Wi-Fi and Bluetooth capabilities eliminate the need for external communication modules, reducing the overall footprint and power consumption of the measurement node. The ESP32's robust FreeRTOS operating system ensures deterministic execution of critical sampling routines. At the same time, its ample SRAM (520 KB) facilitates

the local buffering of high-resolution electrical data during intermittent network outages, thereby preventing data loss in harsh industrial environments.

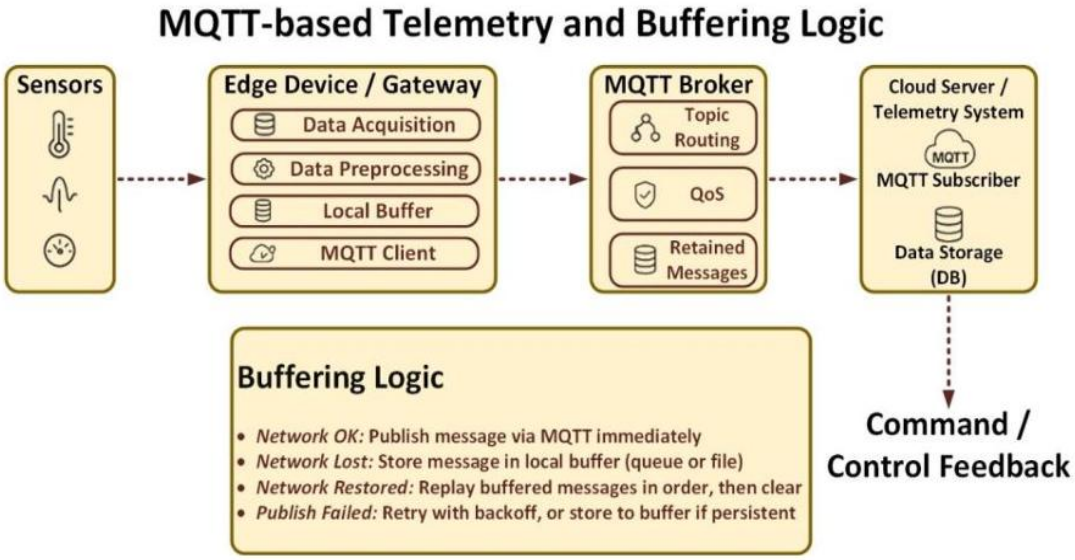



**Fig. 3:** MQTT-based telemetry and buffering scheme showing the data flow from sensors through edge device/gateway to MQTT broker and cloud server.

It interfaces directly with the ADE9000 via SPI to acquire the high-resolution electrical data. The ESP32 performs initial data buffering, basic signal validation, and packetization. Crucially, it manages the MQTT communication stack, ensuring secure (TLS) and reliable data transmission to the cloud infrastructure over Wi-Fi or cellular networks. Its dual-core architecture allows for concurrent data acquisition and network management, minimizing latency and preventing data loss during intermittent connectivity.

## 2.3. Hybrid Anomaly and Prediction Pipeline

The server-side data flow, outlined in Figure 4, feeds into a two-stage modeling pipeline that separates process periodicity and trends as “normal behavior” and then measures the sequential anomaly density in the residual signals.

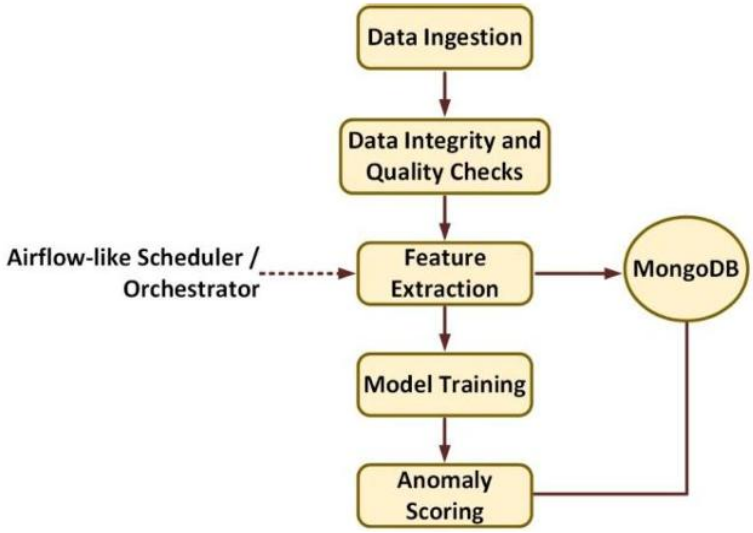



**Fig. 4:** Server-side data flow diagram illustrating the sequential processing pipeline from data ingestion through feature extraction, model training, and anomaly scoring.

As outlined in the complete hybrid pipeline architecture given in Figure 5, the first stage utilizes Prophet to produce a residual series by separating trend and seasonality components in each critical attribute or attribute set; thus, shift cycles, weekday/weekend differences, and rhythms dependent on the production plan are included in the normal component. In the second stage, an LSTM-based sequence model learns short- to medium-term dependencies in these residual sequences, producing an anomaly density score for each time step.

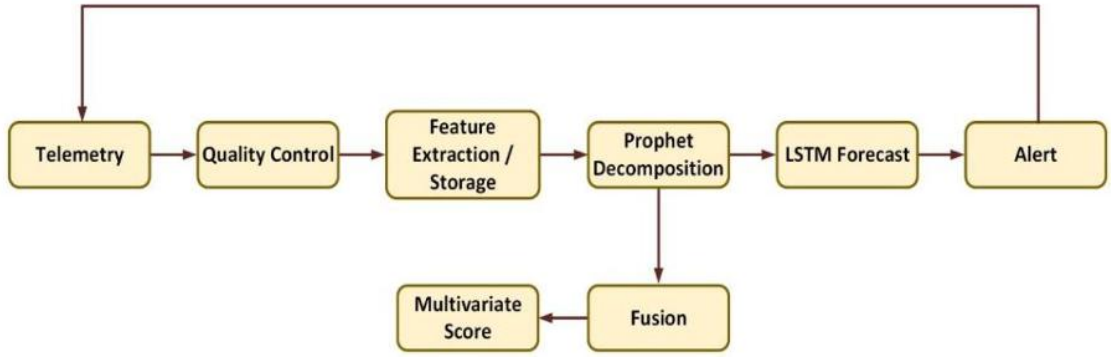



**Fig. 5:** The complete hybrid pipeline architecture combining telemetry acquisition, quality control, feature extraction, Prophet decomposition, LSTM forecasting, multivariate scoring, and fusion-based alert generation.

To strengthen the multivariate context, deviations from the joint distribution of selected features within the same window are calculated in parallel using an intensity- or distance-based metric (e.g., covariance-normalized Mahalanobis distance). Finally, score fusion combines these two sources (sequential and multivariate) to create a single anomaly metric; alerts and maintenance actions are mapped based on dynamic thresholds determined by field validation.

### *2.3.1. Prophet Algorithm*

The Prophet algorithm is a decomposable time-series forecasting model designed to capture trend, seasonality, and special event effects within an additive framework. It is particularly suitable for industrial time-series data due to its robustness to missing values, outliers, and irregular sampling intervals [34].

The general formulation of Prophet is given as:

$$y(t) = g(t) + s(t) + h(t) + \varepsilon_t \quad (1)$$

where $g(t)$ shows the trend component, $s(t)$ is the seasonal component, $h(t)$ represents the holiday or event effects, and $\varepsilon_t$ is the error term.

Trend and seasonality decomposition with Prophet is performed within an additive model framework, and the observed series is represented as the sum of trend, seasonality, and special-day/event effects, as shown in Eq. 1.

The trend component of the Prophet is typically modeled as a piecewise linear function as given in Eq. 2:

$$g(t) = \left(K + \sum_{k=1}^{S} \delta_k \, \mathbb{I}(t \geq \tau_k)\right) t + \left(\beta + \sum_{k=1}^{S} \gamma_k \, \mathbb{I}(t \geq \tau_k)\right) \quad (2)$$

where $K$ is the initial growth rate, $\delta_k$ shows the rate adjustments at change points, $\tau_k$ is the change point locations, $\beta$ is the offset, and $\gamma_k$ represents adjustment parameters.

Piecewise linear or sigmoidal trends are flexibly captured with breakpoints determined by the data; daily and weekly seasonality is modeled using Fourier bases, which compactly express recurring patterns. This approach allows rhythms commonly observed in energy consumption and production processes to be transferred to the normal component, thereby increasing the residual's anomaly sensitivity.

When multiple attributes are involved, Prophet is applied to individual channels or meaningful groups; residual signals derived from these channels are then stacked along the time axis to form input for the sequential model. Prophet's tolerance for missing samples controls data irregularities that are inevitable in field conditions, while Fourier degrees and smoothing coefficients are adjusted through cross-validation to prevent overfitting [35]. In this work, Prophet is used to model normal system behavior by capturing trend and periodic patterns in electrical features (e.g., load cycles, operational schedules).

### *2.3.2. LSTM Algorithm*

The Long Short-Term Memory (LSTM) is a type of recurrent neural network (RNN) designed to model long-term temporal dependencies through gated memory structures. It effectively mitigates the vanishing gradient problem encountered in conventional RNNs [36].

At each time step $t$, the LSTM cell is defined by the following equations:

$$\text{Forget Gate } f_t = \sigma\left(W_f x_t + U_f h_{t-1} + b_f\right) \quad (3)$$

$$\text{Input Gate } i_t = \sigma(W_i x_t + U_i h_{t-1} + b_i) \quad (4)$$

$$\text{Candidate Memory } \tilde{c}_t = \tanh(W_c x_t + U_c h_{t-1} + b_c) \quad (5)$$

$$\text{Cell State Update } c_t = f_t \odot c_{t-1} + i_t \odot \tilde{c}_t \quad (6)$$

$$\text{Output Gate } o_t = \sigma(W_o x_t + U_o h_{t-1} + b_o) \quad (7)$$

$$\text{Hidden state } h_t = o_t \odot \tanh(c_t) \quad (8)$$

where $x_t$ is the input vector, $h_t$ is the hidden state, $c_t$ is the cell state, $\sigma$ shows sigmoid activation, and $\odot$ represents element-wise multiplication.

The LSTM component uses gated memory structures to capture temporal dependencies in residual signals and quantifies anomalies via prediction error using a one-step-ahead forecasting approach. The model learns typical dynamics by being trained in an unsupervised or semi-supervised manner with normal operating windows; in real-time inference, the expected residual is generated for each new step, and the difference between it and the observed value is scaled by the error covariance and converted into an anomaly score [37].

Inter-channel scale differences in multi-channel data streams are eliminated using z-score normalization; the window size is selected by balancing alarm delay and score stability. As the field distribution changes over time, periodic retraining and versioning strategies help maintain model performance; Huber-like losses and early stopping are used to enhance robustness.

Finally, the hybrid pipeline combines these two sources—namely, the LSTM's sequential error-based score and the multivariate deviation score from the same window—to produce a single anomaly metric. The scores are scaled to a percentile-based range and combined using weighted fusion; the weights are adjusted based on the field's early-warning requirements and false-alarm tolerance. Following the fusion, the decision layer evaluates both the score and its gradient to classify alerts into three levels: immediate intervention, planned maintenance, and monitoring. Along with the decision, a report details which features contributed most to the score and where deviations were observed in which harmonic bands or imbalance indicators, for explainability purposes. Thus, not only the probability of failure but also actionable insights regarding energy efficiency and power quality are presented to the user.

In the proposed framework, LSTM operates on residual sequences obtained from Prophet. It learns temporal dependencies in these residuals and performs one-step-ahead forecasting. This hybrid approach is particularly effective in industrial PdM scenarios where both interpretability and predictive performance are critical.

The LSTM network employed in this study is designed to process the Prophet residuals. The architecture consists of an input layer, two hidden LSTM layers, and a dense output layer. Specific parameters are as follows:

• Input Layer: Accepts sequences of Prophet residuals, with a look-back window of 30 time steps (e.g., 30 previous residual values).

• Hidden Layer 1: 64 LSTM units, followed by a Dropout layer with a rate of 0.2 to prevent overfitting.

• Hidden Layer 2: 32 LSTM units, followed by a Dropout layer with a rate of 0.2.

• Activation Function: Rectified Linear Unit (ReLU) for the LSTM layers.

• Output Layer: A single dense unit with a linear activation function, predicting the next residual value.

• Optimizer: Adam optimizer with a learning rate of 0.001.

• Loss Function: Mean Squared Error (MSE).

• Batch Size: 64.

• Epochs: 100, with early stopping if validation loss does not improve for 10 consecutive epochs.

This configuration allows the LSTM to effectively learn the underlying patterns in the residual series, enabling accurate prediction of normal residual behavior and, consequently, robust anomaly detection when actual residuals deviate significantly from predictions.

### *2.3.2. Hybrid Prophet-LSTM Framework*

Anomaly detection in the hybrid Prophet-LSTM framework is based on quantifying the deviation of observed data from the model's predictions. The process involves several steps:

- Prophet Residuals: The Prophet model first forecasts the expected behavior of the time series. The difference between the actual observed values and the Prophet's predictions yields the residuals. These residuals represent the unmodeled, potentially anomalous components of the data.

- LSTM Prediction Error: The LSTM model is then trained on these historical residuals to learn their normal temporal dynamics. During inference, the LSTM predicts the next residual value based on a sequence of previous residuals. The anomaly score for the LSTM component is calculated as the absolute difference between the actual residual and the LSTM's predicted residual (i.e., the LSTM prediction error).

- Thresholding: A dynamic threshold is applied to the LSTM prediction error. This threshold is typically determined using statistical methods (e.g., the 3-sigma rule or a percentile-based approach) based on the distribution of prediction errors under normal operating conditions. Values exceeding this threshold are flagged as potential anomalies.

- Fusion Score: To provide a comprehensive anomaly indicator, a fusion score is computed by combining multiple anomaly signals. In this study, the primary anomaly signal is the LSTM prediction error. Additionally, we incorporate deviations in key electrical parameters (e.g., sudden spikes in THD, significant phase imbalance) that are not fully captured by the time-series models but are known indicators of faults. The fusion score is calculated as a weighted sum of the normalized LSTM prediction error and the normalized deviations of these critical electrical parameters. The weights are determined empirically based on expert knowledge and historical fault data, giving greater weight to indicators with stronger correlations to specific fault types. For instance, a high LSTM prediction error combined with an elevated 5th harmonic trend would result in a higher fusion score, indicating a strong likelihood of bearing degradation.

# 3. Experimental Setup and Results

## 3.1. Industrial Deployment

The proposed AI-driven predictive maintenance system (MIOTE) was tested on critical cooling group motors in an industrial facility. Electrical data from two asynchronous motors with similar nominal powers and operating conditions (hereafter referred to as “Motor A” and “Motor B”) were collected and analyzed over a 4-month period (May-September).

The system monitored parameters such as voltage (V), current (I), harmonics (THD), power factor, and phase imbalances at sub-second resolution, running rule-based and AI-based anomaly detection algorithms in parallel. To facilitate real-time monitoring and decision-making, a dedicated web-based dashboard was developed within the MIOTE framework, as shown in Figure 6. The dashboard provides comprehensive visualization of electrical parameters, harmonic content, power quality indicators, anomaly scores, energy losses, and estimated carbon emissions. It enables maintenance personnel to track asset performance, identify emerging faults, and evaluate the economic and environmental impacts of detected inefficiencies through an intuitive graphical interface.




**Fig. 6:** MIOTE monitoring dashboard. (a) Energy efficiency, performance, and $CO_2$ emission analysis (b) Electrical parameter and power quality monitoring

## 3.2. Harmonic Analysis and Mechanical Fault Correlation

Figure 7 illustrates the harmonic behavior of Motor A over the four-month monitoring period. Spectral analyses conducted on Motor A revealed that the Total Harmonic Distortion of Current

(THDI) values frequently hovered around 36%. While voltage THD values remained stable at the 2% level, this elevation in current harmonics indicated load-induced non-linearities rather than electrical pollution.

Notably, significant increasing trends and time-based fluctuations were detected in the 5th and 11th harmonics, which are negative sequence harmonics. It is known in the literature that negative sequence harmonics create a torque opposite to the rotor rotation direction. When the heat maps and trend analyses generated by the system were examined, it was concluded that these harmonics pointed to rotating component problems such as bearing wear, journal sliding, or cage path deformation. This data demonstrates that the system can detect not only electrical but also mechanical faults using the Electrical Signature Analysis (ESA) method.

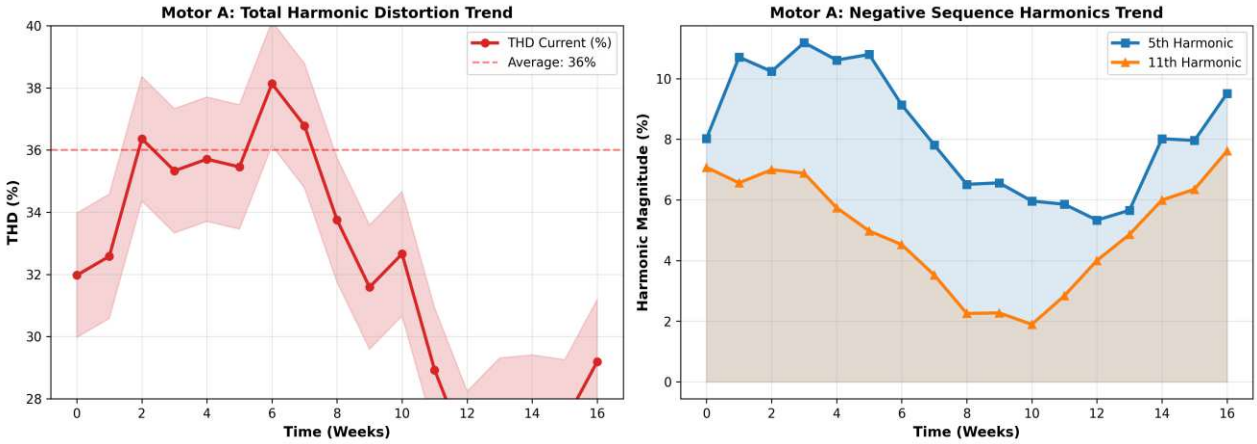



**Fig. 7:** Harmonic analysis trend for Motor A over the 4-month monitoring period, highlighting the elevated THD and specific negative sequence harmonics (5th and 11th).

Table 1 summarizes the harmonic analysis findings, detailing the correlation between specific harmonic orders and mechanical faults. and their corresponding mechanical fault correlations.

**Table 1:** Summary of harmonic analysis and mechanical fault correlation for Motor A.

| Parameter | Observed Value | Normal Range | Fault Indication | Recommended Action |
|---|---|---|---|---|
| Voltage THD | ~2.0% | < 5.0% | Normal grid condition | None |
| Current THD (THDI) | ~36.0% | < 10.0% | Load-induced non-linearity | Install a passive filter |
| 5th Harmonic | Increasing Trend | Stable | Negative sequence torque | Inspect bearings/journal |
| 11th Harmonic | Increasing Trend | Stable | Negative sequence torque | Inspect the cage path |

## 3.3. Phase Imbalances and Connection Anomalies

When the Motor B data were examined, it was determined that the inter-phase current imbalance ranged from 3.6% to 9.5%, as shown in Figure 8. Although the voltage imbalance was negligible

(below 0.8%), the high current imbalance indicated that the problem did not originate from the grid.

In the correlation analyses performed, it was observed that when the voltage difference increased, the current difference decreased, or the characteristic of the imbalance did not change with loading. This situation revealed that the problem stemmed from increased transition resistance due to winding resistance differences, corrosion, or loose connections, rather than rotor or mechanical friction.

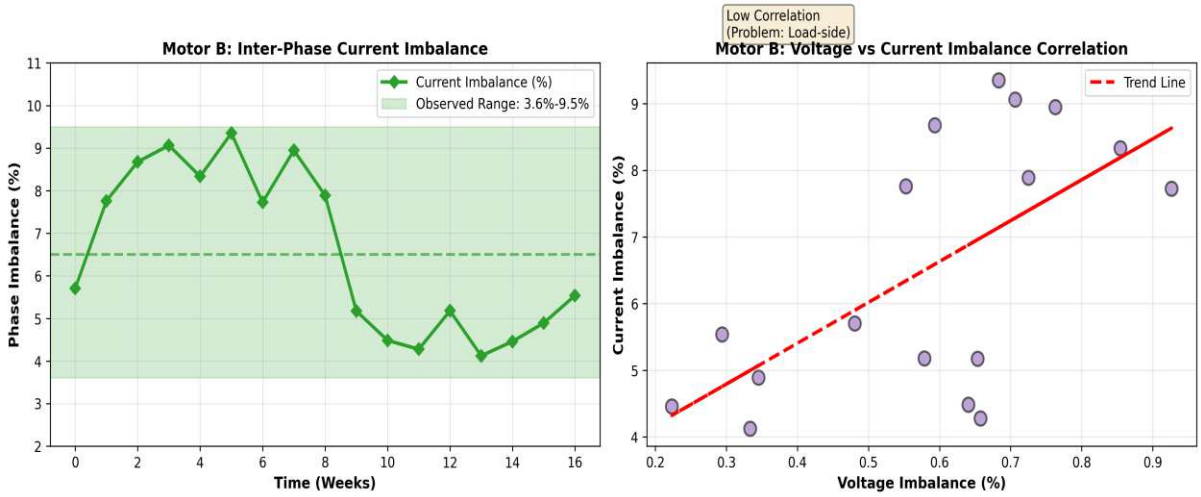



**Fig. 8:** Phase imbalance analysis for Motor B, showing the current imbalance trend and its correlation with voltage imbalance.

## 3.4. Drive (VFD) Performance and Starting Current Analysis

Contrary to the soft-start characteristic expected in Variable Frequency Drive (VFD) systems, it was detected that the starting currents of Motor B reached 3 to 4 times the nominal current. This value, which should normally be at the 1.5In level, indicates that the drive parameters (ramp time, V/f curve) were configured incorrectly or that insulation weakness had begun in the stator windings. The system labeled this anomaly as “critical” and presented a parameter optimization recommendation to the maintenance teams.

## 3.5. Energy Efficiency and Carbon Footprint Analysis

The developed system calculated the economic and environmental cost of the detected electrical inefficiencies (harmonic losses and phase imbalances). Figure 9 presents the estimated annual $CO_2$ emissions and energy losses associated with the electrical inefficiencies detected in Motor A and Motor B.

- **Motor A:** It was calculated that the losses created by high harmonics (36% THDI) added an inefficiency to the system equivalent to approximately 27-28 tons of CO2 emissions annually.
- **Motor B:** It was determined that the losses caused by phase imbalances caused approximately 12 tons of CO2 emissions annually.

The system reported that an efficiency increase of over 5% could be achieved by applying a passive filter to Motor A, while energy savings could be achieved by revising the connection for Motor B.

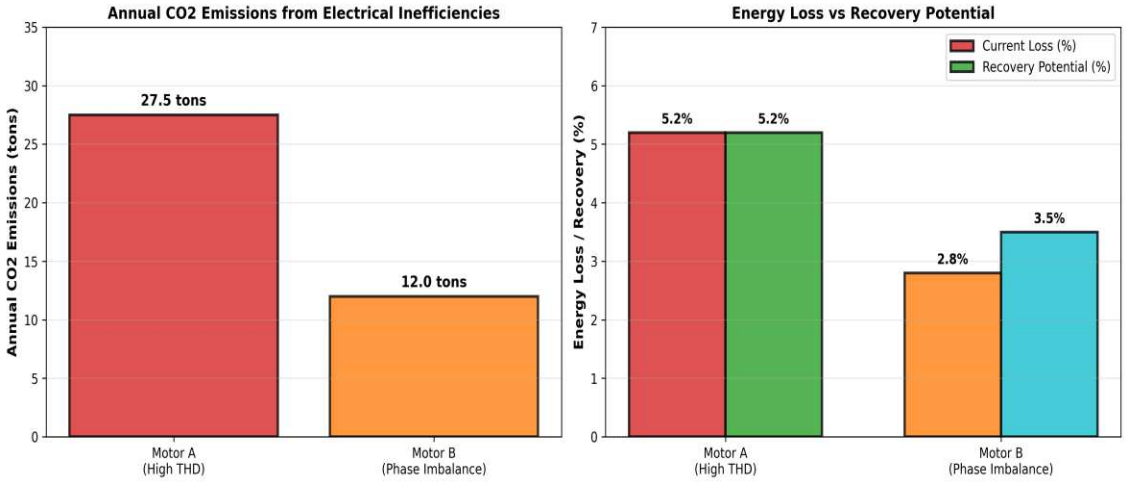



**Fig. 9:** Estimated annual CO2 emissions and energy loss percentages due to electrical inefficiencies in Motor A and Motor B.

Table 2 presents the energy-efficiency analysis and the corresponding environmental impact.

**Table 2:** Energy efficiency and carbon footprint analysis for the monitored motors.

| Motor | Primary Inefficiency | Energy Loss (%) | Annual CO2 Emissions (Tons) | Proposed Solution | Expected Recovery (%) |
|---|---|---|---|---|---|
| Motor A | High Harmonics (36% THDI) | 5.2% | 27.5 | Passive Filter Application | > 5.0% |
| Motor B | Phase Imbalance (3.6-9.5%) | 2.8% | 12.0 | Connection Revisions | ~ 3.5% |

## 3.6. Anomaly Detection Performance: AI vs. Rule-Based

During the four-month monitoring period, the "Artificial Intelligence (AI)" module produced more sensitive results than traditional "Rule-Based" alarms. For example, while rule-based systems only generate alarms when threshold values are exceeded (e.g., I > Limit), the AI module detected deviations in harmonic trends and departures from normal operating conditions (baseline) at a much earlier stage, lowering the "Performance Index" and providing early warning. The fact that the number of AI-originated anomalies in the reported periods was significantly higher than rule-based alarms, and that these anomalies coincided with field controls (looseness, bearing noise, etc.), confirms the success of the algorithm.

The AI-driven module demonstrated significant efficacy in early fault detection, outperforming traditional rule-based alarms. Table 3 summarizes the performance metrics for the hybrid Prophet-LSTM model compared to a baseline rule-based system.

**Table 3:** Performance Comparison of Anomaly Detection Systems

| Anomaly Detection System | Accuracy | Precision | Recall | F1-Score |
|---|---|---|---|---|
| Rule-Based System | 0.78 | 0.69 | 0.65 | 0.67 |
| Hybrid Prophet-LSTM | 0.94 | 0.92 | 0.90 | 0.91 |

The results clearly indicate that the hybrid Prophet-LSTM model achieves substantially higher accuracy, precision, recall, and F1-score, highlighting its superior capability in identifying incipient faults with fewer false positives and false negatives. This robust performance is attributed to the model's ability to learn complex temporal dependencies in the residuals, effectively distinguishing subtle anomalous patterns from normal operational variations.

## 3.7. Ablation Study

To demonstrate the effectiveness of the hybrid Prophet-LSTM approach, an ablation study was conducted to compare its performance with individual Prophet and LSTM models. The models were evaluated using the same dataset and metrics as described in Section 2.3.

**Table 4:** Ablation Study Results for Anomaly Detection

| Anomaly Detection Algorithms | Accuracy | Precision | Recall | F1-Score |
|---|---|---|---|---|
| Rule-Based | 0.78 | 0.69 | 0.65 | 0.67 |
| LSTM Only | 0.81 | 0.77 | 0.75 | 0.76 |
| Prophet Only | 0.84 | 0.78 | 0.75 | 0.77 |
| **Hybrid Prophet-LSTM** | 0.94 | 0.92 | 0.90 | 0.91 |

The results from Table 4 clearly indicate that the hybrid Prophet-LSTM model significantly outperforms both standalone Prophet and LSTM models across all evaluation metrics. The Prophet-only model, while providing a good baseline for trend forecasting, struggles to detect nuanced anomalies in the residuals. The LSTM-only model outperforms Prophet due to its ability to capture temporal dependencies. Still, it remains limited by strong trends and seasonality in the raw data, which can mask subtle anomalies. The hybrid approach, by leveraging Prophet to detrend and deseasonalize the data, allows the LSTM to focus exclusively on residual patterns, leading to a marked improvement in anomaly-detection capabilities. This ablation study confirms that the synergistic combination of Prophet and LSTM is crucial for achieving the superior performance observed in this framework.

# 4. Discussion

The experimental results validate the efficacy of the proposed integrated IoT-based PdM framework. The ability to correlate specific harmonic signatures (e.g., the 5th and 11th harmonics) with mechanical degradation underscores the potential of high-resolution electrical monitoring as

a comprehensive diagnostic tool, thereby reducing reliance on supplementary vibration sensors. Furthermore, the identification of loose connections via phase imbalance analysis highlights the system's sensitivity to subtle electrical anomalies that might otherwise go unnoticed until catastrophic failure.

## 4.1. Comparative Analysis of the Hybrid Prophet-LSTM Approach

The comparative analysis of the AI-driven module and traditional rule-based systems demonstrates the superior early-warning capabilities of the hybrid Prophet-LSTM approach. By establishing dynamic baselines and analyzing residual sequences, the AI module successfully identified incipient faults before threshold breaches, enabling proactive maintenance interventions. This finding aligns with recent studies highlighting the limitations of static rule-based expert systems in dynamic industrial environments [38]. While rule-based systems are easier to implement, they often suffer from high false-alarm rates or missed detections when operating conditions fluctuate.

The integration of Prophet and LSTM leverages the complementary strengths of both architectures. Prophet effectively isolates macroscopic trends and seasonalities (e.g., production shifts, load cycles), while LSTM captures the complex, non-linear temporal dependencies within the residual signals. Similar hybrid architectures have been successfully applied in related domains, such as sales forecasting and energy consumption prediction, demonstrating enhanced data reliability and model readiness [39], [40], [41]. In the context of industrial PdM, this hybrid approach not only improves predictive accuracy but also provides crucial interpretability—a feature often lacking in pure "black-box" deep learning models.

## 4.2. Electrical Signature Analysis vs. Conventional Modalities

The proposed framework emphasizes the utility of Electrical Signature Analysis (ESA) combined with deep learning for comprehensive fault detection. Traditional approaches heavily rely on vibration and thermal monitoring, which, while effective, often require intrusive sensor installations and face scalability challenges. Our results demonstrate that high-resolution electrical monitoring can detect both electrical (e.g., phase imbalance) and mechanical (e.g., bearing wear) faults. This is consistent with recent literature indicating that ESA can serve as a robust predictive maintenance tool for detecting common faults at an early stage, thereby preventing catastrophic failures [42]. Furthermore, the application of deep learning models (such as LSTM and 1D-CNN) to Motor Current Signature Analysis (MCSA) has been shown to yield high diagnostic accuracy for induction motor faults [43].

The deployment of this intelligence at the edge, facilitated by the ESP32 microcontroller, further enhances the system's responsiveness. Edge-based machine learning minimizes latency and reduces the bandwidth required for continuous cloud transmission, a critical advantage in industrial settings with intermittent connectivity [44].

## 4.3. Energy Efficiency and Environmental Impact

Moreover, quantifying energy inefficiencies in terms of CO2 emissions provides a compelling economic and environmental justification for adopting advanced PdM systems. The estimated annual savings of 27-28 tons of CO2 for a single motor emphasize the significant role of electrical asset optimization in industrial decarbonization efforts. This dual focus on reliability and sustainability addresses a critical gap in existing PdM literature, where energy performance

optimization is often treated as a secondary objective rather than an integrated component of the decision-making framework.

## 5. Conclusion

This paper presented an integrated IoT-based Predictive Maintenance framework for industrial electrical assets, leveraging high-resolution electrical signatures and a hybrid deep learning approach. The system's deployment on critical cooling group motors demonstrated its capability to detect both electrical and electromechanical faults, including bearing degradation and loose connections, at an early stage. The AI-driven anomaly detection module outperformed traditional rule-based methods, providing actionable insights for maintenance optimization. Additionally, the system's ability to quantify energy losses and associated carbon emissions highlights its contribution to industrial energy efficiency.

Electrical and harmonic signatures inherently encode coupled electromechanical phenomena: rotor asymmetry manifests as characteristic sideband frequencies; air-gap eccentricity alters the spectral energy distribution; winding faults influence negative-sequence currents; supply anomalies elevate Total Harmonic Distortion (THD) and degrade power factor, thereby inflating $I^2R$ losses and lowering efficiency. A high-precision measurement subsystem—targeting compliance with IEC 61000-4-30 Class S (and scalable toward Class A where feasible) and relevant national technical specifications—provides a trustworthy foundation for early anomaly discernment. In the proposed system, a high-rate sampling front end (8 kHz effective sampling rate, enabling resolution of the fundamental and targeted harmonic bands) acquires raw voltages and currents across phases. From these raw streams, a structured feature hierarchy is built: approximately 67 primary measured electrical quantities (RMS currents/voltages per phase, active/reactive/apparent power components, fundamental frequency, phase angles, power factor, THD for current and voltage, selected individual harmonic magnitudes) are expanded—via spectral decomposition, statistical windowing, and engineered ratios—into up to 328 derived features representing condition, load behavior, and efficiency indicators. This layered representation supports both rapid anomaly scoring and medium-term degradation trend modeling without requiring vibration or thermal sensors in the initial deployment phase.

Future work will focus on expanding the dataset across diverse industrial applications and refining the prognostic models for Remaining Useful Life (RUL) estimation.

## References


[1] S. Aguayo-Tapia, G. Avalos-Almazan, J. de J. Rangel-Magdaleno, and J. M. Ramirez-Cortes, "Physical Variable Measurement Techniques for Fault Detection in Electric Motors," *Energies*, vol. 16, no. 12, 2023, doi: 10.3390/en16124780.

[2] A. Allal and A. Khechekhouche, "Diagnosis of induction motor faults using the motor current normalized residual harmonic analysis method," *Int. J. Electr. Power Energy Syst.*, vol. 141, no. April, p. 108219, 2022, doi: 10.1016/j.ijepes.2022.108219.

[3] K. Hamani, M. Kuchar, M. Kubatko, and S. Kirschner, "Advancements in Induction Motor Fault Diagnosis and Condition Monitoring: A Comprehensive Review," *Sensors*, vol. 25, no. 19, pp. 1–36, 2025, doi: 10.3390/s25195942.

[4] A. Raza, A. Benrabah, T. Alquthami, and M. Akmal, "A review of fault diagnosing methods in power transmission systems," *Appl. Sci.*, vol. 10, no. 4, 2020, doi: 10.3390/app10041312.

[5] W. Elmasry and M. Wadi, "Enhanced Anomaly-Based Fault Detection System in Electrical Power Grids," *Int. Trans. Electr. Energy Syst.*, vol. 2022, pp. 1–19, 2022, doi: 10.1155/2022/1870136.

[6] L. Xu, S. S. Teoh, and H. Ibrahim, "A deep learning approach for electric motor fault diagnosis based on modified InceptionV3," *Sci. Rep.*, vol. 14, no. 1, pp. 1–15, 2024, doi: 10.1038/s41598-024-63086-9.

[7] V. G. de Araújo *et al.*, "Monitoring and Diagnosing Faults in Induction Motors' Three-Phase Systems Using NARX Neural Network," *Energies*, vol. 17, no. 18, 2024, doi: 10.3390/en17184609.

[8] T. Anwar *et al.*, "Robust fault detection and classification in power transmission lines via ensemble machine learning models," *Sci. Rep.*, vol. 15, no. 1, pp. 1–17, 2025, doi: 10.1038/s41598-025-86554-2.

[9] R. R. Kumar, M. Andriollo, G. Cirrincione, M. Cirrincione, and A. Tortella, "A Comprehensive Review of Conventional and Intelligence-Based Approaches for the Fault Diagnosis and Condition Monitoring of Induction Motors," *Energies*, vol. 15, no. 23, 2022, doi: 10.3390/en15238938.

[10] K. Yatsugi, S. E. Pandarakone, Y. Mizuno, and H. Nakamura, "Common Diagnosis Approach to Three-Class Induction Motor Faults Using Stator Current Feature and Support Vector Machine," *IEEE Access*, vol. 11, no. February, pp. 24945–24952, 2023, doi: 10.1109/ACCESS.2023.3254914.

[11] B. H. Bahgat, E. A. Elhay, and M. M. Elkholy, "Advanced fault detection technique of three phase induction motor: comprehensive review," *Discov. Electron.*, vol. 1, no. 1, 2024, doi: 10.1007/s44291-024-00012-3.

[12] R. Hussain, M. A. Saleh, and S. S. Refaat, "Various Faults Classification of Industrial Application of Induction Motors Using Supervised Machine Learning: A Comprehensive Review," *IEEE Access*, vol. 13, no. August, pp. 146649–146675, 2025, doi:

10.1109/ACCESS.2025.3600570.

[13] S. Akbar, T. Vaimann, B. Asad, A. Kallaste, M. U. Sardar, and K. Kudelina, “State-of-the-Art Techniques for Fault Diagnosis in Electrical Machines: Advancements and Future Directions,” *Energies*, vol. 16, no. 17, 2023, doi: 10.3390/en16176345.

[14] S. Gawde, S. Patil, S. Kumar, P. Kamat, K. Kotecha, and A. Abraham, “Multi-fault diagnosis of Industrial Rotating Machines using Data-driven approach : A review of two decades of research,” *Eng. Appl. Artif. Intell.*, vol. 123, no. February 2022, p. 106139, 2023, doi: 10.1016/j.engappai.2023.106139.

[15] A. Varghese, J. R. P. K. Ande, R. Mahadasa, S. S. Gutlapalli, and P. Surarapu, “Investigation of Fault Diagnosis and Prognostics Techniques for Predictive Maintenance in Industrial Machinery,” *Eng. Int.*, vol. 11, no. 1, pp. 9–26, 2023, doi: 10.18034/ei.v11i1.693.

[16] S. Singh, A. Kumar, and N. Kumar, “Motor Current Signature Analysis for Bearing Fault Detection in Mechanical Systems,” *Procedia Mater. Sci.*, vol. 6, no. Icmpc, pp. 171–177, 2014, doi: 10.1016/j.mspro.2014.07.021.

[17] H. Lee, H. Kim, J. Jeong, K. Lee, S. Bin Lee, and G. Stone, “Inverter-Embedded Partial Discharge Testing for Reliability Enhancement of Stator Winding Insulation in Low Voltage Machines,” *IEEE Trans. Ind. Appl.*, vol. 58, no. 2, pp. 2088–2096, 2022, doi: 10.1109/TIA.2022.3142712.

[18] P. Balakrishna and U. Khan, “An Autonomous Electrical Signature Analysis-Based Method for Faults Monitoring in Industrial Motors,” *IEEE Trans. Instrum. Meas.*, vol. 70, 2021, doi: 10.1109/TIM.2021.3059466.

[19] L. Biggio and I. Kastanis, “Prognostics and Health Management of Industrial Assets: Current Progress and Road Ahead,” *Front. Artif. Intell.*, vol. 3, no. November, pp. 1–24, 2020, doi: 10.3389/frai.2020.578613.

[20] I. Hector and R. Panjanathan, “Predictive maintenance in Industry 4.0: a survey of planning models and machine learning techniques,” *PeerJ Comput. Sci.*, vol. 10, pp. 1–50, 2024, doi: 10.7717/peerj-cs.2016.

[21] A. Aboshosha, A. Haggag, N. George, and H. A. Hamad, “IoT-based data-driven predictive maintenance relying on fuzzy system and artificial neural networks,” *Sci. Rep.*, vol. 13, no. 1, pp. 1–13, 2023, doi: 10.1038/s41598-023-38887-z.

[22] R. Kumar and R. S. Anand, “Health monitoring and fault analysis of induction motors: a review,” *Eng. Res. Express*, vol. 6, no. 4, 2024, doi: 10.1088/2631-8695/ad8b10.

[23] O. Khattach, O. Moussaoui, and M. Hassine, “End-to-End Architecture for Real-Time IoT Analytics and Predictive Maintenance Using Stream Processing and ML Pipelines,” *Sensors*, vol. 25, no. 9, pp. 1–14, 2025, doi: 10.3390/s25092945.

[24] R. De Luca, A. Ferraro, A. Galli, M. Gallo, V. Moscato, and G. Sperlì, “A deep attention based approach for predictive maintenance applications in IoT scenarios,” *J. Manuf. Technol. Manag.*, vol. 34, no. 4, pp. 535–556, 2023, doi: 10.1108/JMTM-02-2022-0093.

[25] X. Wen, J. Liao, Q. Niu, N. Shen, and Y. Bao, “Deep learning-driven hybrid model for short-term load forecasting and smart grid information management,” *Sci. Rep.*, vol. 14, no. 1, pp. 1–16, 2024, doi: 10.1038/s41598-024-63262-x.

[26] Y. Bouabdallaoui, Z. Lafhaj, P. Yim, L. Ducoulombier, and B. Bennadji, “Predictive maintenance in building facilities: A machine learning-based approach,” *Sensors (Switzerland)*, vol. 21, no. 4, pp. 1–15, 2021, doi: 10.3390/s21041044.

[27] K. Kaushik and V. Naik, “Detecting faults in the cooling systems by monitoring temperature and energy,” *Energy Informatics*, vol. 7, no. 1, pp. 1–27, 2024, doi: 10.1186/s42162-024-00351-1.

[28] Q. Zhou *et al.*, “Enhancing multimodal fault diagnosis in mechanical systems via mixture of experts,” *Complex Intell. Syst.*, vol. 11, no. 10, pp. 1–38, 2025, doi: 10.1007/s40747-025-02061-x.

[29] E. De Santis, F. Arnò, and A. Rizzi, “Estimation of fault probability in medium voltage feeders through calibration techniques in classification models,” *Soft Comput.*, vol. 26, no. 15, pp. 7175–7193, 2022, doi: 10.1007/s00500-022-07194-6.

[30] P. Chakraborty *et al.*, “Smart Power Systems Transformation: Advanced Fault Detection With Edge Computing and Signal Processing in LV Networks With EV Charging Stations,” *IEEE Access*, vol. 13, no. June, pp. 125029–125056, 2025, doi: 10.1109/ACCESS.2025.3586062.

[31] Z. Zamanzadeh Darban, G. I. Webb, S. Pan, C. Aggarwal, and M. Salehi, “Deep Learning for Time Series Anomaly Detection: A Survey,” *ACM Comput. Surv.*, vol. 57, no. 1, 2024, doi: 10.1145/3691338.

[32] Dazok Donald Jambol, Oludayo Olatoye Sofoluwe, Ayemere Ukato, and Obinna Joshua Ochulor, “Transforming equipment management in oil and gas with AI-Driven predictive maintenance,” *Comput. Sci. IT Res. J.*, vol. 5, no. 5, pp. 1090–1112, 2024, doi: 10.51594/csitrj.v5i5.1117.

[33] S. Rana, “Ai-Driven Fault Detection and Predictive Maintenance in Electrical Power Systems: a Systematic Review of Data-Driven Approaches, Digital Twins, and Self-Healing Grids,” *Am. J. Adv. Technol. Eng. Solut.*, vol. 1, no. 01, pp. 258–289, 2025, doi: 10.63125/4p25x993.

[34] S. J. Taylor and B. Letham, “Forecasting at Scale,” *Am. Stat.*, vol. 72, no. 1, pp. 37–45, 2018, doi: 10.1080/00031305.2017.1380080.

[35] O. Kurt, “Model-based prediction of water levels for the Great Lakes: a comparative analysis,” *Earth Sci. Informatics*, vol. 17, no. 4, pp. 3333–3349, 2024, doi: 10.1007/s12145-024-01341-3.

[36] F. Karim, S. Majumdar, H. Darabi, and S. Chen, “LSTM Fully Convolutional Networks for Time Series Classification,” *IEEE Access*, vol. 6, pp. 1662–1669, 2017, doi: 10.1109/ACCESS.2017.2779939.

[37] Y. Baghoussi, C. Soares, and J. Mendes-Moreira, “Corrector LSTM: built-in training data

correction for improved time-series forecasting," *Neural Comput. Appl.*, vol. 36, no. 26, pp. 16213–16231, 2024, doi: 10.1007/s00521-024-09962-x.

[38] M. Khan, M. A. Khan, B. Moser, W. Rafique, X. Xiaolong, and D. Wanchun, "AI-Driven Predictive Maintenance in Industrial IoTs: A Comprehensive Survey," *IEEE Internet Things J.*, vol. 13, no. 10, pp. 20275–20298, 2026, doi: 10.1109/JIOT.2026.3660780.

[39] S. Arslan, "A hybrid forecasting model using LSTM and Prophet for energy consumption with decomposition of time series data," *PeerJ Comput. Sci.*, vol. 8, no. 2020, 2022, doi: 10.7717/PEERJ-CS.1001.

[40] S. Albahli, "LSTM vs. Prophet: Achieving Superior Accuracy in Dynamic Electricity Demand Forecasting," *Energies*, vol. 18, no. 2, 2025, doi: 10.3390/en18020278.

[41] M. Milli, "Designing a residual-enhanced hybrid Prophet–LSTM framework for urban air pollution forecasting in Beijing," *Sci. Rep.*, vol. 15, no. 1, pp. 1–24, 2025, doi: 10.1038/s41598-025-27510-y.

[42] P. Cocca, M. Gökan, V. Pesenti, E. Stefana, R. Bortolani, and D. Romagnoli, "Anomaly detection using electrical signature analysis and machine learning: application to a CNC mill," *IFAC-PapersOnLine*, vol. 58, no. 8, pp. 139–144, 2024, doi: 10.1016/j.ifacol.2024.08.063.

[43] M. Hussain, T. D. Memon, I. Hussain, Z. A. Memon, and D. Kumar, "Fault Detection and Identification Using Deep Learning Algorithms in Induction Motors," *C. - Comput. Model. Eng. Sci.*, vol. 133, no. 2, pp. 435–470, 2022, doi: 10.32604/cmes.2022.020583.

[44] J. de las Morenas, F. Moya-Fernández, and J. A. López-Gómez, "The Edge Application of Machine Learning Techniques for Fault Diagnosis in Electrical Machines," *Sensors*, vol. 23, no. 5, 2023, doi: 10.3390/s23052649.